Aalborg Universitet

AALBORG UNIVERSITY
DENMARK

Plug-and-Play Voltage/Current Stabilization DC Microgrid Clusters with Grid-Forming/Feeding Converters

Han, Renke; Tucci, Michele; Martinelli, Andrea; Guerrero, Josep M.; Ferrari-Trecate, Giancarlo

Plug-and-Play Voltage/Current Stabilization DC Microgrid Clusters with Grid-Forming/Feeding Converters

Renke Han[1], *Student Member, IEEE,* Michele Tucci[2], *Student Member, IEEE,* Andrea Martinelli[3],
Josep M. Guerrero[1], *Fellow, IEEE,* Giancarlo Ferrari-Trecate[4], *Senior Member, IEEE*

Abstract— In this paper, we propose a new decentralized control scheme for Microgrid (MG) clusters, given by the interconnection of atomic dc MGs, each composed by grid-forming and grid-feeding converters. In particular, we develop a new Plug-and-Play (PnP) voltage/current controller for each MG in order to achieve simultaneous voltage support and current feeding function with local references. The coefficients of each stabilizing controller are characterized by explicit inequalities, which are related only to local electrical parameters of the MG. With the proposed controller, each MG can plug-in/out of the clusters seamlessly irrespectively of the power line parameters and models of other MGs. A profound proof of closed-loop stability of MG clusters is provided. Moreover, theoretical results are validated by hardware-in-loop (HiL) tests.

I. INTRODUCTION

During the past decades, dc MGs have been recognized more and more attractive compared with ac MG [1], as they provide a higher efficiency, more natural interface. Grid-forming converters are used as the interface between energy storage system (ESSes) and the system to provide voltage support in dc MGs. To achieve simultaneous voltage support and communication-less current sharing among ESSes, voltage-current (V-I) or I-V droop control [2], [3] is widely adopted by imposing virtual impedance for output voltages. However, voltage deviations and current sharing errors cannot be eliminated due to different line impedances. Another key challenge is that the stability of connected ESSes is sensitive to the chosen virtual impedances which should be designed taking into account the specific MG topologies [4], [5], [6]. Recently, an alternative class of decentralized primary controllers, called PnP controller according to the terminology used in [7], has been proposed in [8], [9], [10]. In [10], to achieve PnP robust voltage control, information about line impedances need be known to form the upper and lower boundary for system model. On the other hand, PnP controllers in [8], [9] form a decentralized control architecture where each regulator can be synthesized using information about the corresponding ESSes only [9] or, at most, specific parameters of the power lines connected to the

ESSes [8]. The latter pieces of information are not required in the design procedure of [9], which is therefore termed line-independent method.

However, for the PnP methods mentioned above, the synthesis of a PnP controller requires to solve a convex optimization problem, and if it is unfeasible, the plug-in/out of corresponding ESS must be denied. Moreover, they are only suited for grid-forming converters, as they provide only voltage support in the system. However, one complete MG must be composed of renewable energy source(RESes), ESSes and loads to achieve the power generation, storage and consumption. When RESes such as PV sources are added in dc MGs, grid-feeding converters should be used as the interface to achieve current feeding for the system according to the reference given by e.g. maximum power point tracking algorithm [11]. Furthermore the current stabilization should be guaranteed. In [12], a current-based PI primary droop control is proposed considering the constant current load. Then, a current-based PnP controller is proposed for grid-feeding converters [13]. The joint utilization of grid-feeding and grid-forming converters has been considered for studying energy management problems [14], [15], [16]. However, from the stability point of view, if the grid-forming and grid-feeding converters are considered simultaneously, the controller and its stability should be redesigned. To authors' knowledge, the stabilization of MG clusters including both types of converters has never been considered before, independently of the number of MGs and the topologies.

In this paper, considering a MG cluster, a PnP voltage/current controller is proposed to achieve voltage support and current feeding functions simultaneously. The set of coefficients of each local controller is explicitly characterized through a set of inequalities which only depends on the local parameters. In particular, we show that controller design is always feasible and does not require to solve an optimization problem. Global closed-loop stability is formally proven.

The paper is structured as follows. In Section II and III-A, the model of a MG cluster and the proposed controller are introduced. In Section III-B, the global closed-loop stability is proven. Finally, the HiL tests are shown in Section IV.

II. DC MGS WITH GRID-FORMING/FEEDING CONVERTERS

A. Electrical model of MGs

A MG composed of one grid-forming converter and one grid-feeding converter connected to a single point of common

[1]R. Han and J. M. Guerrero is with Department of Energy Technology, Aalborg University, Aalborg, Denmark {rha,joz}@et.aau.dk

[2]M. Tucci is with Dipartimento di Ingegneria Industriale e dell'Informazione, Università degli Studi di Pavia, Pavia, Italy michele.tucci02@universitadipavia.it

[3]A. Martinelli is with Dipartimento di Elettronica, Informazione e Bioingegneria, Politecnico di Milano, Milano, Italy andrea5.martinelli@mail.polimi.it

[4] G. Ferrari-Trecate is with Automatic Control Laboratory, École Polytechnique Fédérale de Lausanne (EPFL), Lausanne, Switzerland giancarlo.ferraritrecate@epfl.ch

coupling (PCC) bus is considered achieving both voltage support and current feeding.

A MG cluster is obtained by interconnecting N MGs, induced by the set $\mathcal{D} = \{1, \ldots, N\}$. Two MGs are neighbors if there is a power line connecting them and denote with $\mathcal{N}_i \subset \mathcal{D}$ the subset of neighbors of MG i. The neighboring relation is symmetric which means $j \in \mathcal{N}_i$ implies $i \in \mathcal{N}_j$. Furthermore, let $\mathcal{E} = \{(i,j) : i \in \mathcal{D}, j \in \mathcal{N}_i\}$ collect unordered pairs of indices associated to lines. The topology of the MG cluster is then described by the undirected graph $\mathcal{G}_{el}$ with nodes $\mathcal{D}$ and edges $\mathcal{E}$. The electrical scheme of the i-th MG is illustrated in left block of Fig. 1.

$$\text{MG } i : \begin{cases} \dfrac{dV_i}{dt} = \dfrac{1}{C_{ti}} I_{ti}^C + \dfrac{1}{C_{ti}} I_{ti}^V + \sum_{j \in \mathcal{N}_i} \left(\dfrac{V_j}{C_{ti} R_{ij}} - \dfrac{V_i}{C_{ti} R_{ij}} \right) \\ \qquad - \dfrac{1}{C_{ti}} (I_{Li} + \dfrac{V_i}{R_{Li}}) \\ \dfrac{dI_{ti}^C}{dt} = -\dfrac{1}{L_{ti}^C} V_i - \dfrac{R_{ti}^C}{L_{ti}^C} I_{ti}^C + \dfrac{1}{L_{ti}^C} V_{ti}^C \\ \dfrac{dI_{ti}^V}{dt} = -\dfrac{1}{L_{ti}^V} V_i - \dfrac{R_{ti}^V}{L_{ti}^V} I_{ti}^V + \dfrac{1}{L_{ti}^V} V_{ti}^V \end{cases} \quad (1)$$

where variables V_i, I_{ti}^C, I_{ti}^V are the i-th PCC voltage, filter current from RES and filter current from ESS, respectively. For the grid-feeding converter, V_{ti}^C represents the command and R_{ti}^C, L_{ti}^C are the electrical parameters. For the grid-forming converter, V_{ti}^V represents the command and R_{ti}^V, L_{ti}^V are the electrical parameters; C_{ti} is the capacitor at the PCC bus. Moreover, V_j is the voltage at the PCC of each neighboring MGs $j \in \mathcal{N}_i$ and R_{ij} and L_{ij} are the resistance and inductance of the dc power line connecting MGs i and j. In general, the RL parameters are different for grid-feeding and grid-forming converters.
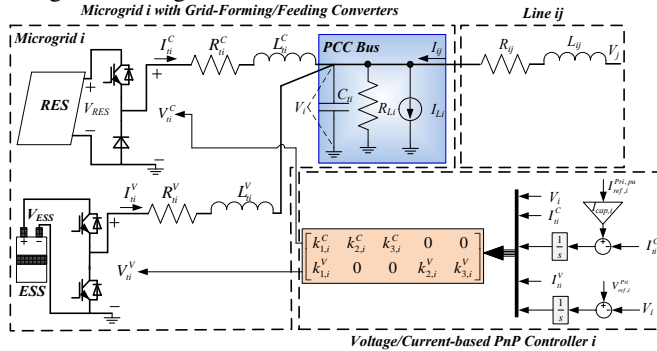

Fig. 1: Electrical Scheme of MG i with PnP Voltage/Current Controller.

B. State-space model of MG Clusters

Dynamics (1) provides the state-space model:

$$\Sigma_{[i]}^{MG} : \begin{cases} \dot{x}_{[i]}(t) = A_{ii} x_{[i]}(t) + B_i u_{[i]}(t) + M_i d_{[i]}(t) \\ \qquad + \xi_{[i]}(t) + A_{load,i} x_{[i]}(t) \\ z_{[i]}(t) = H_i x_{[i]}(t) \end{cases}$$

where $x_{[i]} = [V_i, I_{ti}^C, I_{ti}^V]^T$ is the state of the system, $u_{[i]} = [V_{ti}^C, V_{ti}^V]$ is the control input, $d_{[i]} = I_{Li}$ is the exogenous input and $z_{[i]} = [I_i^C, V_i]$ is the controlled variable. The term $\xi_{[i]} = \sum_{j \in \mathcal{N}_i} A_{ij}(x_{[j]} - x_{[i]})$ accounts for the coupling with each MG $j \in \mathcal{N}_i$. The matrices of $\Sigma_{[i]}^{MG}$ are obtained from (1). The details about matrices can be found in [17].

The overall model for a MG cluster is given by

$$\begin{aligned} \dot{\mathbf{x}}(t) &= \mathbf{A}\mathbf{x}(t) + \mathbf{B}\mathbf{u}(t) + \mathbf{M}\mathbf{d}(t) \\ \mathbf{z}(t) &= \mathbf{H}\mathbf{x}(t) \end{aligned} \quad (2)$$

where $\mathbf{x} = (x_{[1]}, \ldots, x_{[N]}) \in \mathbb{R}^{3N}$, $\mathbf{u} = (u_{[1]}, \ldots, u_{[N]}) \in \mathbb{R}^{2N}$, $\mathbf{d^C} = (d_{[1]}, \ldots, d_{[N]}) \in \mathbb{R}^N$, $\mathbf{z} = (z_{[1]}, \ldots, z_{[N]}) \in \mathbb{R}^{2N}$. Matrices $\mathbf{A}$, $\mathbf{B}$, $\mathbf{M}$ and $\mathbf{H}$ are reported in Appendix A in [17].

III. DESIGN OF STABILIZING VOLTAGE/CURRENT CONTROLLERS

A. Structure of PnP Voltage/Current controllers

In order to track constant references $\mathbf{z_{ref}}(t)$, when $\mathbf{d}(t)$ is constant as well, the MG model is augmented with integrators [18]. A necessary condition for making error $\mathbf{e}(t) = \mathbf{z_{ref}}(t) - \mathbf{z}(t)$ equal to zero as $t \to \infty$, is that, for arbitrary $\bar{\mathbf{d}}$ and $\bar{\mathbf{z}}_{\mathbf{ref}}$, there are equilibrium states and inputs $\bar{\mathbf{x}}$ and $\bar{\mathbf{u}}$ verifying (2). The existence of these equilibrium points can be shown as in the proof of Proposition 1 in [8].

Let $I_{cap,i} > 0$ define the maximal output current capability provided by MG i. According to the block on the bottom right of Fig. 1, the dynamics of integrators are given by

$$\begin{cases} \dot{v}_{[i]}^C(t) = e_{[i]}^C(t) = z_{ref_{[i]}}^{Pri,C}(t) - I_{ti}^C(t) & (3a) \\ \dot{v}_{[i]}^V(t) = e_{[i]}^V(t) = z_{ref_{[i]}}^{Pri,V}(t) - V_i(t) & (3b) \end{cases}$$

where $z_{ref_{[i]}}^{Pri,C} = I_{ref,i}^{Pri,pu} * I_{cap,i}$, $z_{ref_{[i]}}^{Pri,V} = V_{ref,i}^{Pri}$,
Hence, the augmented MG model is

$$\hat{\Sigma}_{[i]}^{MG} : \begin{cases} \dot{\hat{x}}_{[i]}(t) = \hat{A}_{ii} \hat{x}_{[i]}(t) + \hat{B}_i u_{[i]}(t) + \hat{M}_i \hat{d}_{[i]}(t) \\ \qquad + \hat{\xi}_{[i]}(t) + \hat{A}_{load,i} \hat{x}_{[i]}(t) \\ z_{[i]}(t) = \hat{H}_i \hat{x}_{[i]}(t) \end{cases} \quad (4)$$

where $\hat{x}_{[i]} = [V_i, I_{ti}^C, v_i^C, I_{ti}^V, v_i^V]^T \in \mathbb{R}^5$ is the state, $\hat{d}_{[i]} = [d_{[i]}, z_{ref_{[i]}}^{Pri,C}, z_{ref_{[i]}}^{Pri,V}]^T \in \mathbb{R}^3$ collects the exogenous signals and $\hat{\xi}_{[i]} = \sum_{j \in \mathcal{N}_i} \hat{A}_{ij}(\hat{x}_{[j]} - \hat{x}_{[i]})$. Matrices in (4) can be established by combining (1) with (3).

Based on Proposition 2 in [8], it can be proven that the pair $(\hat{A}_{ii}, \hat{B}_i)$ is controllable. Hence, system (4) can be stabilized.

The overall augmented system is obtained from (4) as

$$\begin{cases} \dot{\hat{\mathbf{x}}}(t) = \hat{\mathbf{A}}\hat{\mathbf{x}}(t) + \hat{\mathbf{B}}\mathbf{u}(t) + \hat{\mathbf{M}}\hat{\mathbf{d}}(t) \\ \mathbf{z}(t) = \hat{\mathbf{H}}\hat{\mathbf{x}}(t) \end{cases} \quad (5)$$

where $\hat{\mathbf{x}}$ and $\hat{\mathbf{d}}$ collect variables $\hat{x}_{[i]}$ and $\hat{d}_{[i]}$ respectively, and matrices $\hat{\mathbf{A}}, \hat{\mathbf{B}}, \hat{\mathbf{M}}$ and $\hat{\mathbf{H}}$ are obtained from systems (4).

Each MG $\hat{\Sigma}_{[i]}^{MG}$ is with the following state-feedback controller

$$\mathcal{C}_{[i]}^{MG} : \qquad u_{[i]}(t) = K_i \hat{x}_{[i]}(t) \quad (6)$$

where

$$K_i = \begin{bmatrix} k_{1,i}^C & k_{2,i}^C & k_{3,i}^C & 0 & 0 \\ k_{1,i}^V & 0 & 0 & k_{2,i}^V & k_{3,i}^V \end{bmatrix} \in \mathbb{R}^{2 \times 5}.$$

Noting that the control variables V_{ti}^C and V_{ti}^V are coupled through the coefficients $k_{1,i}^C$ and $k_{1,i}^V$ appearing in the first column of K_i. In particular, the overall control architecture is decentralized since the computation of $u_{[i]}$ requires the state of $\hat{\Sigma}_{[i]}^{MG}$ only.

B. Conditions for stability of the closed-loop MG Cluster

For showing stability, we will use local Lyapunov functions

$$V_i(\hat{x}_{[i]}) = [\hat{x}_{[i]}]^T P_i \hat{x}_{[i]}. \tag{7}$$

Assumption 1. *The positive definite matrix $P_i \in \mathbb{R}^{5\times5}$ in (7) fulfills*

$$P_i = \left[\begin{array}{c|c|c} \eta_i & \mathbf{0}_{1\times2} & \mathbf{0}_{1\times2} \\ \hline \mathbf{0}_{2\times1} & \mathcal{P}^C_{22,i} & \mathbf{0}_{2\times2} \\ \hline \mathbf{0}_{2\times1} & \mathbf{0}_{2\times2} & \mathcal{P}^V_{44,i} \end{array}\right], \tag{8}$$

where

$$\mathcal{P}^C_{22,i} = \begin{bmatrix} p^C_{22,i} & p^C_{23,i} \\ p^C_{23,i} & p^C_{33,i} \end{bmatrix}, \mathcal{P}^V_{44,i} = \begin{bmatrix} p^V_{44,i} & p^V_{45,i} \\ p^V_{54,i} & p^V_{55,i} \end{bmatrix}. \tag{9}$$

And $\eta_i > 0$ is a local parameter satisfying $\eta_i = \bar{\sigma}C_{ti}$, $i \in \mathcal{D}$ where $\bar{\sigma} > 0$ is a constant parameter, common to all MGs.

In absence of coupling terms $\hat{\xi}_{[i]}(t)$, and load terms $\hat{A}_{load,i}\hat{x}_{[i]}(t)$, we would like to guarantee asymptotic stability of the nominal closed-loop MG

$$\dot{\hat{x}}_{[i]}(t) = \underbrace{(\hat{A}_{ii} + \hat{B}_i K_i)}_{F_i}\hat{x}_{[i]}(t) + \hat{M}_i\hat{d}_{[i]}(t). \tag{10}$$

By direct calculation, one can show that F_i has the following structure

$$F_i = \left[\begin{array}{c|cc|cc} 0 & f_{12,i} & 0 & f_{14,i} & 0 \\ \hline f_{21,i} & f_{22,i} & f_{23,i} & 0 & 0 \\ 0 & f_{32,i} & 0 & 0 & 0 \\ \hline f_{41,i} & 0 & 0 & f_{44,i} & f_{45,i} \\ f_{51,i} & 0 & 0 & 0 & 0 \end{array}\right]$$

$$= \left[\begin{array}{c|cc|cc} 0 & \frac{1}{C_{ti}} & 0 & \frac{1}{C_{ti}} & 0 \\ \hline \frac{(k^C_{1,i}-1)}{L^C_{ti}} & \frac{(k^C_{2,i}-R^C_{ti})}{L^C_{ti}} & \frac{k^C_{3,i}}{L^C_{ti}} & 0 & 0 \\ 0 & -1 & 0 & 0 & 0 \\ \hline \frac{(k^V_{1,i}-1)}{L^V_{ti}} & 0 & 0 & \frac{(k^V_{2,i}-R^V_{ti})}{L^V_{ti}} & \frac{k^V_{3,i}}{L^V_{ti}} \\ -1 & 0 & 0 & 0 & 0 \end{array}\right] \tag{11}$$

$$= \left[\begin{array}{c|c|c} 0 & \mathcal{F}^C_{12,i} & \mathcal{F}^V_{14,i} \\ \hline \mathcal{F}^C_{21,i} & \mathcal{F}^C_{22,i} & 0 \\ \hline \mathcal{F}^V_{41,i} & 0 & \mathcal{F}^V_{44,i} \end{array}\right].$$

From Lyapunov theory, asymptotic stability of (10) can be certified by the existence of a Lyapunov function $\mathcal{V}_i(\hat{x}_{[i]}) = [\hat{x}_{[i]}]^T P_i \hat{x}_{[i]}$ where $P_i = P_i^T > 0$ and

$$Q_i = F_i^T P_i + P_i F_i \tag{12}$$

is negative definite. In presence of nonzero coupling terms, we will show that asymptotic stability can be achieved under Assumption 1.

Based on (8) and (11), (12) can be rewritten as (13) shown in the upper part of the next page.

Next, we provide two lemmas and two propositions by which we can analyze the closed-loop system and parametrize explicitly the set of stabilizing controllers.

Lemma 1. *Under Assumption 1, if $Q_i \leq 0$, $Q_i \in \mathbb{R}^{5\times5}$ has the following structure*

$$Q_i = \left[\begin{array}{c|c|c} 0 & \mathbf{0}_{1\times2} & \mathbf{0}_{1\times2} \\ \hline \mathbf{0}_{2\times1} & \mathcal{Q}^C_{22,i} & \mathbf{0}_{2\times2} \\ \hline \mathbf{0}_{2\times1} & \mathbf{0}_{2\times2} & \mathcal{Q}^V_{44,i} \end{array}\right] \tag{14}$$

Furthermore, the blocks on the diagonal must verify

$$\begin{cases} \mathcal{Q}^C_{22,i} \leq 0 & \text{(15a)} \\ \mathcal{Q}^C_{44,i} \leq 0 & \text{(15b)} \end{cases}$$

Proof. See the proof of Lemma 2 in [17]. □

Remark 1. *Since the blocks $\mathcal{Q}^C_{22,i}$ and $\mathcal{Q}^V_{44,i}$ belong to $\mathbb{R}^{2\times2}$, from (15), the determinants of $\mathcal{Q}^C_{22,i}$ and $\mathcal{Q}^V_{44,i}$ are nonnegative.*

Proposition 1. *[9] If $Q = Q^T \leq 0$ and an element q_{ii} on the diagonal are verified $q_{ii} = 0$, then*

(i) The matrix Q cannot be negative definite.

(ii) The i-th row and column of Q have zero entries.

Proposition 2. *Under Assumption 1, matrices P_i and Q_i have the structure given in (16) (displayed in the upper part of next page), where $h_i = L^V_{ti}k^V_{3,i} - (k^V_{1,i} - 1)(k^V_{2,i} - R^V_{ti})$. Moreover, if $P_i > 0$, $Q_i \leq 0$ and $Q_i \neq 0$, one has*

$$\begin{cases} k^C_{1,i} < 1 \\ k^C_{2,i} < R^C_{ti} \\ k^C_{3,i} > 0 \end{cases}, \begin{cases} k^V_{1,i} < 1 \\ k^V_{2,i} < R^V_{ti} \\ 0 < k^V_{3,i} < \frac{1}{L^V_{ti}}(k^V_{1,i} - 1)(k^V_{2,i} - R^V_{ti}) \end{cases} \tag{17}$$

Proof. See proof of Proposition 4 in [17]. □

Lemma 2. *Let Assumptions 1 and Proposition 2 hold, define $h_i(v_i) = v_i^T \mathcal{Q}^V_{44,i} v_i$, with $v_i \in \mathbb{R}^2$. If $Q_i \leq 0$, and $Q_i \neq 0$, then*

$$h_i(\bar{v}_i) = 0 \Longleftrightarrow \bar{v}_i \in \text{Ker}(\mathcal{F}^V_{44,i}).$$

Proof. See the proof of Proposition 3 in [9]. □

Proposition 3. *Let $g_i(w_i) = w_i^T Q_i w_i$, $\forall i \in \mathcal{D}$ with $w_i \in \mathbb{R}^5$. Under Assumption 1, Proposition 2, and Lemma 2, only vectors $\bar{w}_i$ in the form*

$$\bar{w}_i = \begin{bmatrix} \alpha_i & 0 & \gamma_i & \beta_i & \delta_i\beta_i \end{bmatrix}^T$$

with α_i, γ_i, $\beta_i \in \mathbb{R}$, and $\delta_i = -\frac{k^V_{2,i}-R^V_{ti}}{k^V_{3,i}}$, fulfill

$$g_i(\bar{w}_i) = \bar{w}_i^T Q_i \bar{w}_i = 0. \tag{18}$$

Proof. See proof of Proposition 5 in [17]. □

Consider the overall closed-loop MG cluster model

$$\begin{cases} \dot{\hat{x}}(t) = (\hat{\mathbf{A}} + \hat{\mathbf{B}}\mathbf{K})\hat{x}(t) + \hat{\mathbf{M}}\hat{\mathbf{d}}(t) \\ \mathbf{z}(t) = \hat{\mathbf{H}}\hat{x}(t) \end{cases} \tag{19}$$

$$Q_i = \begin{bmatrix} 0 & [\mathcal{F}_{21,i}^C]^T \mathcal{P}_{22,i}^C + \eta_i \mathcal{F}_{12,i}^C & [\mathcal{F}_{41,i}^V]^T \mathcal{P}_{44,i}^V + \eta_i \mathcal{F}_{14,i}^V \\ [\mathcal{F}_{12,i}^C]^T \eta_i + \mathcal{P}_{22,i}^C \mathcal{F}_{21,i}^C & [\mathcal{F}_{22,i}^C]^T \mathcal{P}_{22,i}^C + \mathcal{P}_{22,i}^C \mathcal{F}_{22,i}^C & \mathbf{0}_{2\times2} \\ [\mathcal{F}_{14,i}^V]^T \eta_i + \mathcal{P}_{44,i}^V \mathcal{F}_{41,i}^V & \mathbf{0}_{2\times2} & [\mathcal{F}_{44,i}^V]^T \mathcal{P}_{44,i}^V + \mathcal{P}_{44,i}^V \mathcal{F}_{44,i}^V \end{bmatrix} = \begin{bmatrix} 0 & \mathcal{Q}_{12,i}^C & \mathcal{Q}_{14,i}^V \\ [\mathcal{Q}_{12,i}^C]^T & \mathcal{Q}_{22,i}^C & \mathbf{0}_{2\times2} \\ [\mathcal{Q}_{14,i}^V]^T & \mathbf{0}_{2\times2} & \mathcal{Q}_{44,i}^V \end{bmatrix} \tag{13}$$

$$P_i = \begin{bmatrix} \eta_i & 0 & 0 & 0 & 0 \\ 0 & p_{22,i}^C & 0 & 0 & 0 \\ 0 & 0 & \frac{k_{3,i}^C}{L_{ti}^C} p_{22,i}^C & 0 & 0 \\ 0 & 0 & 0 & \frac{L_{ti}^V}{C_{ti}^V}\frac{(k_{2,i}^V - R_{ti}^V)}{h_i} & \frac{L_{ti}^V}{C_{ti}}\frac{k_{3,i}^V}{h_i} \\ 0 & 0 & 0 & \frac{L_{ti}^V}{C_{ti}}\frac{k_{3,i}^V}{h_i} & \frac{1}{C_{ti}}\frac{k_{3,i}^V(k_{1,i}^V-1)}{h_i} \end{bmatrix}, Q_i = \begin{bmatrix} 0 & 0 & 0 & 0 & 0 \\ 0 & 2\frac{(k_{2,i}^C - R_{ti}^C)}{L_{ti}^C} p_{22,i}^C & 0 & 0 & 0 \\ 0 & 0 & 0 & 0 & 0 \\ 0 & 0 & 0 & 2\frac{(k_{2,i}^V - R_{ti}^V)^2}{C_{ti}h_i} & 2\frac{(k_{2,i}^V - R_{ti}^V)k_{3,i}^V}{C_{ti}h_i} \\ 0 & 0 & 0 & 2\frac{(k_{2,i}^V - R_{ti}^V)k_{3,i}^V}{C_{ti}h_i} & 2\frac{(k_{3,i}^V)^2}{C_{ti}h_i} \end{bmatrix} \tag{16}$$

obtained by combining (5) and (6), with $\mathbf{K} = \mathrm{diag}(K_1, \ldots, K_N)$. Considering also the collective Lyapunov function

$$\mathcal{V}(\hat{\mathbf{x}}) = \sum_{i=1}^N \mathcal{V}_i(\hat{x}_{[i]}) = \hat{\mathbf{x}}^T \mathbf{P} \hat{\mathbf{x}} \tag{20}$$

where $\mathbf{P} = \mathrm{diag}(P_1, \ldots, P_N)$. One has $\dot{\mathcal{V}}(\hat{\mathbf{x}}) = \hat{\mathbf{x}}^T \mathbf{Q} \hat{\mathbf{x}}$ where

$$\mathbf{Q} = (\hat{\mathbf{A}} + \hat{\mathbf{B}}\mathbf{K})^T \mathbf{P} + \mathbf{P}(\hat{\mathbf{A}} + \hat{\mathbf{B}}\mathbf{K}). \tag{21}$$

A consequence of Proposition 1 is that, under Assumption 1, the matrix $\mathbf{Q}$ cannot be negative definite. At most, one has

$$\mathbf{Q} \le 0. \tag{22}$$

Moreover, even if $Q_i \le 0$ holds for all $i \in \mathcal{D}$, the inequality (22) might be violated because of the nonzero coupling terms $\hat{A}_{ij}$ and load terms $\hat{A}_{load,i}$ in matrix $\hat{\mathbf{A}}$. The next result shows that this cannot happen.

In order to derive that $Q_i \le 0$, $\forall i \in \mathcal{D}$ implies (22), the following decomposition of matrix $\hat{\mathbf{A}}$ is considered

$$\hat{\mathbf{A}} = \hat{\mathbf{A}}_\mathbf{D} + \hat{\mathbf{A}}_\mathbf{\Xi} + \hat{\mathbf{A}}_\mathbf{L} + \hat{\mathbf{A}}_\mathbf{C}, \tag{23}$$

where $\hat{\mathbf{A}}_\mathbf{D} = \mathrm{diag}(\hat{A}_{ii}, \ldots, \hat{A}_{NN})$ collects the local dynamics only, $\hat{\mathbf{A}}_\mathbf{C}$ collects the coupling dynamic representing the off-diagonal items of matrix $\hat{\mathbf{A}}$. Moreover, matrices $\hat{\mathbf{A}}_\mathbf{\Xi} = \mathrm{diag}(\hat{A}_{\xi1}, \ldots, \hat{A}_{\xi N})$ and $\hat{\mathbf{A}}_\mathbf{L} = \mathrm{diag}(\hat{A}_{load,1}, \ldots, \hat{A}_{load,N})$, where

$$\hat{A}_{\xi i} = \begin{bmatrix} -\sum_{j \in \mathcal{N}_i} \frac{1}{R_{ij}C_{ti}} & \mathbf{0}_{1\times4} \\ \mathbf{0}_{4\times1} & \mathbf{0}_{4\times4} \end{bmatrix}, \hat{A}_{load,i} = \begin{bmatrix} -\frac{1}{R_{Li}C_{ti}} & \mathbf{0}_{1\times4} \\ \mathbf{0}_{4\times1} & \mathbf{0}_{4\times4} \end{bmatrix},$$

take into account the dependence of each local state on the neighboring MGs and the local resistive load respectively. According to the decomposition (23), the inequality (22) is equivalent to

$$\underbrace{(\hat{\mathbf{A}}_\mathbf{D} + \hat{\mathbf{B}}\mathbf{K})^T \mathbf{P} + \mathbf{P}(\hat{\mathbf{A}}_\mathbf{D} + \hat{\mathbf{B}}\mathbf{K})}_{(a)} + \underbrace{2(\hat{\mathbf{A}}_\mathbf{\Xi} + \hat{\mathbf{A}}_\mathbf{L})\mathbf{P}}_{(b)} + \underbrace{\hat{\mathbf{A}}_\mathbf{C}^\mathbf{T}\mathbf{P} + \mathbf{P}\hat{\mathbf{A}}_\mathbf{C}}_{(c)} \le 0 \tag{24}$$

Proposition 4. *If gains K_i are chosen according to (17), then $Q_i \le 0$ for all $i \in \mathcal{D}$, finally (22) holds.*

Proof. See proof of Proposition 6 in [17]. □

Theorem 1. *If Assumptions 1 is fulfilled, the graph $\mathcal{G}_{el}$ is connected, control coefficients are chosen according to (17), then the origin of (5) is asymptotically stable.*

Proof. See proof of Theorem 2 in [17]. □

Remark 2. *The design of stabilizing controller for each MG can be conducted according to Proposition 2. In particular, differently from the approach in [9], no optimization problem has to be solved for computing a local controller. Indeed, it is enough to choose control coefficient $k_{1,i}^C$, $k_{2,i}^C$, $k_{3,i}^C$ and $k_{1,i}^V$, $k_{2,i}^V$, $k_{3,i}^V$ fulfilling the inequalities in (17). Note that these inequalities are always feasible, implying that a stabilizing controller always exists. Moreover, the inequalities depend only on the parameters R_{ti}^C and R_{ti}^V of the MG i. Therefore, the control synthesis is independent of parameters of MGs and power lines, which means that controller design can be executed only once for each converter in a plug-and play fashion.*

IV. HARDWARE-IN-LOOP TEST

In order to verify the correctness of theoretical results, real-time HiL tests have been carried out using dSPACE 1006 platform. The real-time test model comprises four MGs with meshed electrical topology shown in Fig. 2. Meanwhile, the electrical setup information are shown in TABLE I and the transmission lines parameters are shown in TABLE II and the control coefficients are shown in TABLE III

A. Case 1: PnP Test

In this subsection, the effectiveness of the proposed primary PnP controller is verified. Each MG is started separately. At the beginning, we set different voltage and current references for different MGs. The results are shown in Fig. 3. At $t = T1$, MGs $1 - 3$ are connected together without

TABLE I: Electrical setup parameters

Parameter	Symbol	Value
DC source voltage	-	100 V
Nominal voltage	$V_{ref,i}^{Pri}$	48 V
Output capacitance	C_{t*}	2.2 mF
Inductance for CDGU	L_{t*}^{C}	0.018 H
Inductor + switch loss resistance for CDGU	R_{t*}^{C}	0.2 Ω
Inductance for VDGU	L_{t*}^{V}	0.0018 H
Inductor + switch loss resistance for VDGU	R_{t*}^{V}	0.1 Ω
Switching frequency	f_{sw}	10 kHz

TABLE II: Transmission lines parameters

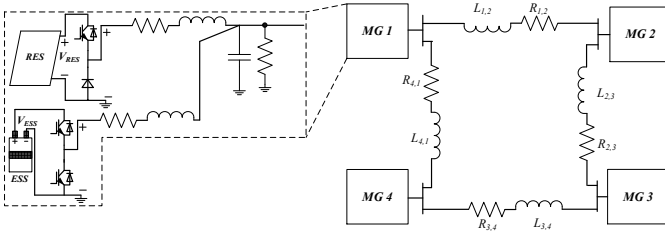| Connected MGs (i,j)	Resistance $R_{i,j}(\Omega)$	Inductance $L_{i,j}(mH)$
$(1,2)$	0.3	1.8
$(2,3)$	0.6	5.4
$(3,4)$	0.8	7.2
$(4,1)$	0.7	3.6

Fig. 2: System Configuration of Hardware-in-Loop Test.

changing the control coefficients. As shown in Fig. 3a, after the connection of MGs $1-3$, only small disturbances appear in the voltage waveform. Moreover, there is no major variation affecting the output currents as shown in Fig. 3b. Then at $t = T2$, MG 4 is connected to the system. Similarly, as shown in Fig. 3, after small disturbance, both the output voltage and current track the respective reference values. Fig.
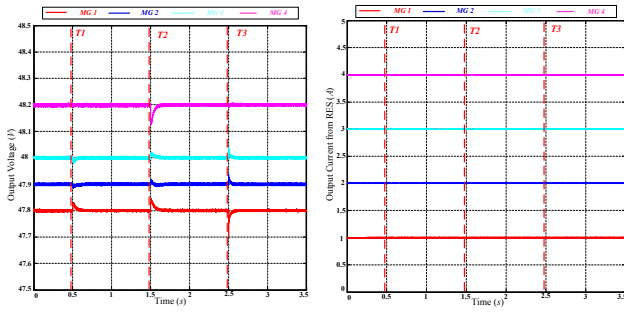

(a) Voltage Performance for PnP Test.

(b) Current Performance for PnP Test.

Fig. 3: The Plug-in/-out Performance of primary PnP controllers.

4 illustrates the current tracking performance by changing the current references for different MGs. At $t = T1$, four MGs are connected together simultaneously. At $t = T2$, the current reference for MG 1 is changed from $1A$ to $2.5A$. At $t = T3$, the current reference for MG 2 is changed from

$2A$ to $3.5A$. At $t = T4$, the current reference for MG 3 is changed from $3A$ to $1.5A$. At $t = T5$, the current reference for MG 4 is changed from $4A$ to $5.5A$. As shown in Fig. 4b, whether the current references are increased or decreased, the output currents can track the changed reference. In addition, as shown in Fig. 4a, when the current references are changed, the output voltages are only affected by little oscillations approximately $0.05V$.
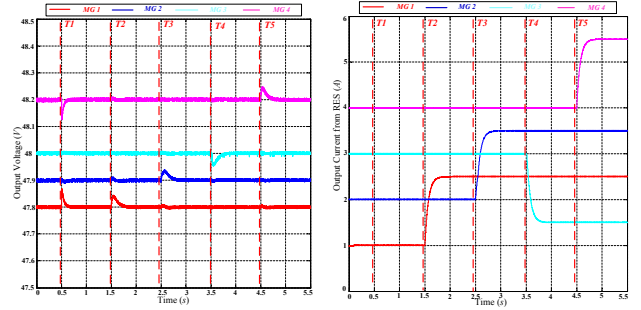
(a) Voltage Tracking Performance.

(b) Current Tracking Performance.

Fig. 4: Voltage and Current Tracking Performance of PnP decentralized controllers

B. Case 2: Instability Test

The correctness and accuracy of coefficient sets in (17) derived from Proposition 2 is verified. According to the system parameters shown in TABLE I, for each MG, the controller coefficients must verify

$$
\begin{cases} k_{1,i}^{C} < 1 \\ k_{2,i}^{C} < 0.2 \\ k_{3,i}^{C} > 0 \end{cases} , \quad
\begin{cases} k_{1,i}^{V} < 1 \\ k_{2,i}^{V} < 0.1 \\ 0 < k_{3,i}^{V} < \dfrac{1}{L_{ti}^{V}}(k_{1,i}^{V} - 1)(k_{2,i}^{V} - R_{ti}^{V}) \end{cases}
\tag{25}
$$

Based on the (25), the value of control coefficients are chosen as shown in Table III. At the beginning, MGs are

TABLE III: Control Coefficients for MG $i = 1,2,3,4$

Control Coefficients	Symbol	Value
For grid-feeding converters	$k_{1,i}^{C}$	-0.01
	$k_{2,i}^{C}$	-2.7015
	$k_{3,i}^{C}$	40.4018
For grid-forming converters	$k_{1,i}^{V}$	-0.480
	$k_{2,i}^{V}$	-0.108
	$k_{3,i}^{V}$	30.673

operated separately and at $t = 0.5s$ MGs are connected together to form the MG cluster. Then at $t = 1s$, the control coefficients are changed in order to violate (25). Fig. 5 including six sub-figures illustrates the system performance when each control coefficient is changed from the stable region to the instable region. Fig. 5a to 5c show that when control coefficients for the grid-forming converter in MG

2 go sightly out of the stable region, the system becomes unstable. Fig. 5d to 5f show that the same happens when control coefficients for the grid-feeding converter in MG 2 slightly violate the inequality.
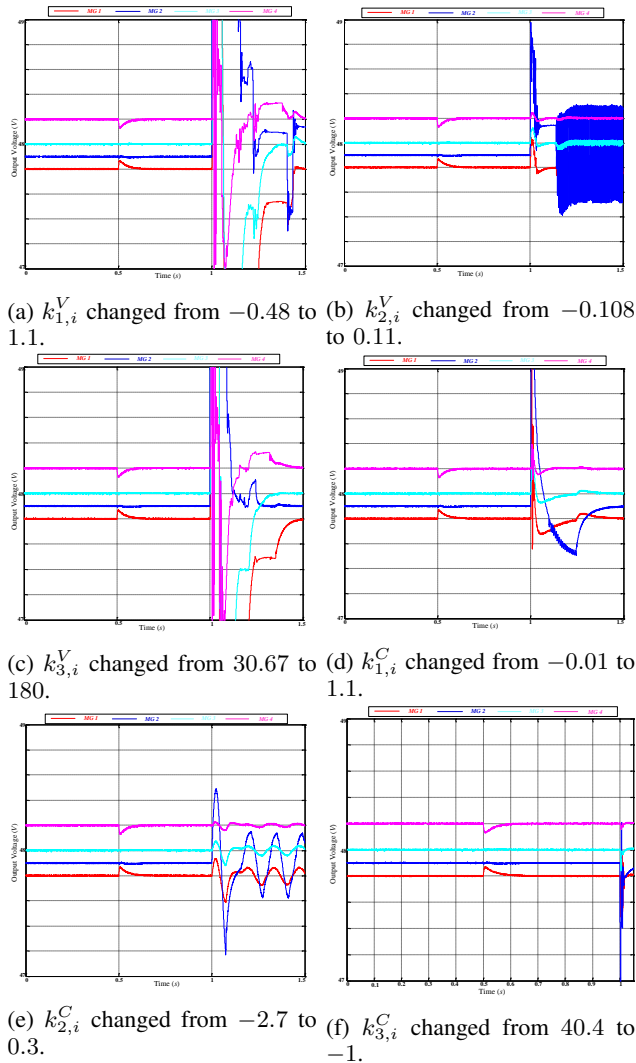

(a) $k_{1,i}^V$ changed from -0.48 to 1.1.

(b) $k_{2,i}^V$ changed from -0.108 to 0.11.

(c) $k_{3,i}^V$ changed from 30.67 to 180.

(d) $k_{1,i}^C$ changed from -0.01 to 1.1.

(e) $k_{2,i}^C$ changed from -2.7 to 0.3.

(f) $k_{3,i}^C$ changed from 40.4 to -1.

Fig. 5: Voltage Profile of Instability Test

V. CONCLUSION

In this paper, a PnP Voltage/Current controller for DC microgrid clusters is proposed. By choosing the control co-efficients according to inequalities which are only related to local parameters, the closed-loop stability can be guaranteed for the MG cluster. Under the proposed control structure, each MG can plug in and out without changing the control coefficients and without knowing the electrical topology of the MG cluster. As in [9], the proofs of closed-loop asymptotic stability exploit structured Lyapunov functions, the LaSalle invariance theorem and properties of graph Laplacians. Thus it shows that these tools offer a feasible theoretical framework for analyzing different kinds of MGs equipped with various types PnP decentralized control architectures. Finally, HiL tests prove the effectiveness and accuracy of the theoretical analysis results.

REFERENCES

[1] R. Han, L. Meng, G. Ferrari-Trecate, E. A. A. Coelho, J. C. Vasquez, and J. M. Guerrero, "Containment and consensus-based distributed coordination control to achieve bounded voltage and precise reactive power sharing in islanded ac microgrids," *IEEE Transactions on Industry Applications*, vol. 53, no. 6, pp. 5187–5199, Nov 2017.

[2] J. M. Guerrero, J. C. Vasquez, J. Matas, D. Vicuna, L. García, and M. Castilla, "Hierarchical control of droop-controlled AC and DC microgrids - A general approach toward standardization," *IEEE Transactions on Industrial Electronics*, vol. 58, no. 1, pp. 158–172, 2011.

[3] R. Han, L. Meng, and J. M. Guerrero, "Hybrid droop control strategy applied to grid-supporting converters in dc microgrids: Modeling, design and analysis," in *IECON 2017 - 43rd Annual Conference of the IEEE Industrial Electronics Society*, Oct 2017, pp. 268–273.

[4] Q. Shafiee, T. Dragičević, J. C. Vasquez, and J. M. Guerrero, "Hierarchical Control for Multiple DC-Microgrids Clusters," *IEEE Transactions on Energy Conversion*, vol. 29, no. 4, pp. 922–933, 2014.

[5] V. Nasirian, S. Moayedi, A. Davoudi, and F. L. Lewis, "Distributed cooperative control of dc microgrids," *IEEE Transactions on Power Electronics*, vol. 30, no. 4, pp. 2288–2303, April 2015.

[6] R. Han, L. Meng, J. M. Guerrero, and J. C. Vasquez, "Distributed non-linear control with event-triggered communication to achieve current-sharing and voltage regulation in dc microgrids," *IEEE Transactions on Power Electronics*, vol. PP, no. 99, pp. 1–1, 2017.

[7] S. Riverso, M. Farina, and G. Ferrari-Trecate, "Plug-and-Play Model Predictive Control based on robust control invariant sets," *Automatica*, vol. 50, no. 8, pp. 2179–2186, 2014.

[8] M. Tucci, S. Riverso, J. C. Vasquez, J. M. Guerrero, and G. Ferrari-Trecate, "A decentralized scalable approach to voltage control of dc islanded microgrids," *IEEE Transactions on Control Systems Technology*, vol. 24, no. 6, pp. 1965–1979, Nov 2016.

[9] M. Tucci, S. Riverso, and G. Ferrari-Trecate, "Line-independent plug-and-play controllers for voltage stabilization in dc microgrids," *IEEE Transactions on Control Systems Technology*, vol. PP, no. 99, pp. 1–9, 2017.

[10] M. S. Sadabadi, Q. Shafiee, and A. Karimi, "Plug-and-play robust voltage control of dc microgrids," *IEEE Transactions on Smart Grid*, vol. PP, no. 99, pp. 1–1, 2017.

[11] C. Kim, Y. Gui, and C. C. Chung, "Maximum power point tracking of a wind power plant with predictive gradient ascent method," *IEEE Transactions on Sustainable Energy*, vol. 8, no. 2, pp. 685–694, April 2017.

[12] J. Zhao and F. Dörfler, "Distributed control and optimization in DC microgrids," *Automatica*, vol. 61, pp. 18–26, 2015.

[13] R. Han, M. Tucci, R. Soloperto, J. M. Guerrero, and G. Ferrari-Trecate, "Plug-and-play design of current controllers for grid-feeding converters in dc microgrids," in *2017 11th Asian Control Conference (ASCC)*, Dec 2017, pp. 2182–2187.

[14] D. Wu, F. Tang, T. Dragicevic, J. M. Guerrero, and J. C. Vasquez, "Coordinated control based on bus-signaling and virtual inertia for islanded dc microgrids," *IEEE Transactions on Smart Grid*, vol. 6, no. 6, pp. 2627–2638, Nov 2015.

[15] X. Zhao, Y. W. Li, H. Tian, and X. Wu, "Energy management strategy of multiple supercapacitors in a dc microgrid using adaptive virtual impedance," *IEEE Journal of Emerging and Selected Topics in Power Electronics*, vol. 4, no. 4, pp. 1174–1185, Dec 2016.

[16] T. Dragicevic, J. M. Guerrero, J. C. Vasquez, and D. Skrlec, "Supervisory control of an adaptive-droop regulated DC microgrid with battery management capability," *IEEE Transactions on Power Electronics*, vol. 29, no. 2, pp. 695–706, Feb 2014.

[17] R. Han, M. Tucci, R. Soloperto, A. Martinelli, G. Ferrari-Trecate, and J. M. Guerrero, "Hierarchical Plug-and-Play Voltage/Current Controller of DC Microgrid Clusters with Grid-Forming/Feeding Converters: Line-independent Primary Stabilization and Leader-based Distributed Secondary Regulation," *ArXiv e-prints*, Jul. 2017.

[18] S. Skogestad and I. Postlethwaite, *Multivariable feedback control: analysis and design*. New York, NY, USA: John Wiley & Sons, 1996.